


# Simulation of the Upper Airways in Patients with Obstructive Sleep Apnea and Nasal Obstruction: A Novel Finite Element Method

Mads Henrik Strand Moxness, MD ; Franziska Wülker, MSc; Bjørn Helge Skallerud, MSc, PhD;  
Ståle Nordgård, MD, PhD

**Objective:** To evaluate the biomechanical properties of the soft palate and velopharynx in patients with obstructive sleep apnea (OSA) and nasal obstruction.

**Study design:** Prospective experimental study.

**Materials and methods:** Two finite element (FE) models of the soft palate were created in six patients undergoing nasal surgery, one homogeneous model based on CT images, and one layered model based on soft tissue composition. The influence of anatomy on displacement caused by a gravitational load and closing pressure were evaluated in both models. The strains in the transverse and longitudinal direction were obtained for each patient.

**Results:** The individual anatomy influences both its structural stiffness and its gravitational displacement. The soft palate width was the sole anatomical parameter correlated to the critical closing pressure, but the maximal displacement due to gravity may have a relationship to closing pressure of possibly an exponential order. The airway occlusion occurred mainly at the lateral attachments of the soft palate. The total transverse strain showed a strong correlation with maximal closing pressure. There was no relationship between the critical closing pressure and the preoperative AHI levels, or the change in AHI after surgery.

**Conclusion:** Hyperelastic FE models both in the homogeneous and layered model represent a novel method of evaluating soft tissue biomechanics of the upper airway. The obstruction occurs mainly at the level of the lateral attachments to the pharyngeal wall, and the width of the soft palate is an indicator of the degree of critical closing pressure. A less negative closing pressure corresponds to small total transverse strain. The effect of nasal surgery on OSA is most likely not explained by change in soft palate biomechanics.

**Key Words:** sleep apnea, nasal obstruction, nasal surgery, upper airways.

**Level of Evidence:** N/A.

## INTRODUCTION

The upper airways may be described as a “critically stable tube” in terms of biomechanics.<sup>1</sup> The balance between the neural drive that enables the dilator muscles to keep the airways open and the counteraction of the intraluminal forces is complex and may be

disrupted if the inward stress of the soft tissues exceeds the airway pressure as demonstrated by hypopneas (airway narrowing) and apnoeas (complete obstruction) in patients suffering from obstructive sleep apnea (OSA). Treatment of OSA ranges from conservative lifestyle restrictions, changes in posture during sleep, positive airway pressure devices and mandibular splints, to extensive surgeries of the upper airways. Surgical treatment of the nasal cavity and velopharynx has frequently been performed because it lowers the intraluminal resistance and facilitates airflow, and results in alterations in soft tissue biomechanical behavior in some patients.<sup>1-3</sup> Successful OSA surgeries are reported,<sup>2,3</sup> but long-term positive outcomes are relatively low<sup>4,5</sup> and most surgeons would emphasize that careful preoperative selection of patients is of key importance.<sup>6</sup> This reflects the lack of standardized treatment and the inability to fully understand the underlying mechanisms that govern the airflow and structural changes in the upper airway during sleep. Our primary aim was to investigate the biomechanical response of the soft palate in OSA using computational finite element (FE) simulations. The secondary aim was to use FE models to evaluate correlations between computational critical closing pressures of the velopharynx and objective OSA measures in patients that underwent nasal surgery. Unlike previous biomechanical studies of the upper airway, we created

This is an open access article under the terms of the Creative Commons Attribution-NonCommercial-NoDerivs License, which permits use and distribution in any medium, provided the original work is properly cited, the use is non-commercial and no modifications or adaptations are made.

From the Department of Otolaryngology, Aleris Hospital, Trondheim, Norway (M.H.S.M); the Department of Neuroscience (M.H.S.M, S.N), Norwegian University of Science and Technology, Trondheim, Norway; the Department of Structural Engineering (F.W., B.H.S.), Norwegian University of Science and Technology, Trondheim, Norway; the Department of Research and Development (F.W.), Duravit AG, Hornberg, Germany; and the Department of Otolaryngology/Head and Neck Surgery (S.N.), St. Olav's University Hospital, Trondheim, Norway

Editor's Note: This Manuscript was accepted for publication 15 January 2018.

Financial disclosure: The project has been funded in part from a grant from the Research council of Norway and a grant from Aleris Hospital, Norway.

Conflict of interest: To our knowledge, there is no conflict of interest.

Send correspondence to Mads Henrik Strand Moxness, Johan Falkbergetsvei 37 7020 Trondheim, Norway. Email: madsmox@gmail.com

DOI: 10.1002/liv.2.140

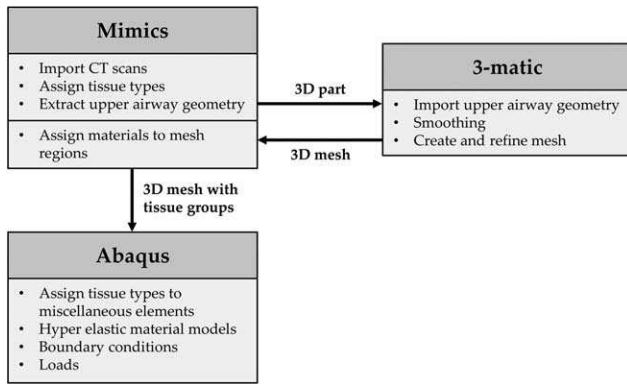


Fig. 1. Workflow of the FE modelling.  
FE = finite element

hyperelastic and histology-based 3D models of the soft palate and velopharynx in order to describe the closing pressure and the soft tissue deformation due to gravity.

## MATERIALS AND METHODS

This prospective controlled study was approved by the Norwegian Ethical Committee and registered in clinicaltrials.gov (NCT01282125). A total of 30 patients with verified OSA by portable polysomnography (Embletta Diagnostic System, ResMed, San Diego, California, U.S.A., and Nox Medical T3, ResMed, Reykjavik, Iceland) and nasal obstruction underwent nasal surgery. We selected six patients with large variations in the anatomy of the soft palate from this cohort to participate in the computational FE simulations. The biomedical engineering program Mimics (Materialise Mimics Innovation Suite, Mimics Research 19.0, Leuven, Belgium) was used to process sagittal, coronal, and axial CT scans and to reconstruct them in 3D geometry. Two different FE models were constructed for each patient, one based on geometric properties of the soft palate (homogeneous model) and one on the soft tissue composition of the soft palate (layered model). A Neo-Hookean material model was employed to account for the soft tissue elasticity. FE simulations were conducted with Abaqus (Abaqus/CAE version 6.14-1, Dassault Systèmes Simulia Corp., Providence, Rhode Island, U.S.A.) in order to compute the maximal displacement of the soft palate as well as the critical closing pressure ( $P_{crit}$ ) at the time of airway occlusion. The workflow of the model generation is displayed in Figure 1. The relation of anatomic measures of the soft palate to its displacement caused by the gravitational and pressure load was investigated to identify anatomical risk factors. In order to predict the effect more accurately we constructed a “shape factor” in which the dependence of the deformation caused by gravitation in more than one anatomic feature is taken into account. As a description of deformation, we calculated three sets of strains in Abaqus: The transverse

strain (from one lateral side to the other, the x-axis, LE11), and the longitudinal strain (from the hard palate to uvula, the y-axis, LE22) and the strain orthogonal to these (z-axis, LE33). All strain components can represent a mix of membrane strain and bending strain, depending on the magnitude of soft palate displacements. The logarithmic (true) strain was used. The following descriptions of computational simulations and material models reflects the emerging new research field of clinical otorhinolaryngology and structural engineering.

MATLAB (MathWorks, version R2015b, The MathWorks, Inc., Natick, Massachusetts, U.S.A.) was used in the statistical analysis to calculate a suitable fit measure (eg, linear) for the anatomic measures using the linear least-squares method. The sum of squares due to error (SSE), the R-square and the root mean squared error (RMSE) was calculated to estimate the goodness of fit. Typically, a small value for SSE and RMSE, and an R-square closer to 1 would indicate a good fit in validating the model with the anatomical measures.

## FE Models

FE models are computational models that provide approximations of partial differential equations (PDE) which are used to describe problems of time or space in physics.<sup>7</sup> FE models of the soft palate and the velopharyngeal airway were created to investigate the influence of anatomical features on the displacement of the soft palate. CT scans with a resolution of 0.46 mm in the x and y direction and 0.7 mm in the z direction were processed in Mimics. Mimics enabled the automatic distinction between bone and soft tissue, while groups of different types of soft tissues had to be selected manually based on literature on histology.<sup>8–11</sup> The modelling domain includes the soft palate from its base at the hard palate to the tip of the uvula and the posterior and lateral walls. The geometry resulting from the tissue segmentation was smoothed using the Materialise module 3-matic (Materialise 3-matic, Research 11.0, Leuven, Belgium). Subsequently, the geometry was meshed with 10-noded tetrahedral elements with a maximum edge length of 1 mm that is a suitable compromise between anatomical accuracy and computational cost caused by the number of elements. The number of elements depends on the shape and size of the soft palate and upper airway and our models consisted of approximately 250,000 elements and one million degrees of freedom.

The homogeneous soft tissue model was utilized to investigate the influence of the macro-anatomy on gravitational loads and pressure. The layered model was used to examine the impact of the different soft tissues that constitutes the soft palate. As no experimental data was available for the soft tissues of the soft palate, material parameters were taken from the literature. For the homogeneous soft tissue model (Table I), parameters describing the overall properties of the soft palate were found in the studies by Birch and Srodon, Pirnar et al., and Yu et al.<sup>12–14</sup> For the layered material model parameters of the soft palate, the material parameters for adipose, glandular, muscular, tendinous, and

TABLE I.  
The Elastic Properties of the Human Soft Palate.

Paper	Material Model	Young’s modulus ( $E$ [Pa])	Poisson ratio ( $\nu$ [-])
Birch and Srodon (2009)	Soft	$9.8 \times 10^2$	0.45
Pirnar et al. (2015)	Medium stiff	$7.54 \times 10^3$	0.49
Yu et al. (2014)	Stiff	$2.5 \times 10^4$	0.42

The Youngs modulus is the stiffness of the material. The Poisson ratio explains the contraction of the soft tissue material when an external pulling force is being exerted.

TABLE II.  
The Elastic Properties of Different Soft Tissues Used in FE Simulations of the Velopharynx.

Model	Paper used	Young's modulus ( $E$ [Pa])	Poisson ratio ( $\nu$ [-])
Adipose soft	Carter et al. (2012)	$5.73 \times 10^2$	0.45
Adipose medium stiff	Ramiao et al. (2016)	$2.74 \times 10^3$	0.45
	Alkhouli et al. (2013)		
	Omidi et al. (2014)		
Adipose stiff	Ramiao et al. (2016)	$2.25 \times 10^4$	0.45
	Carter et al. (2012)		
Bone	Carrigy et al. (2015)	$1.58 \times 10^{10}$	0.35
	Huang et al. (2013)		
	Pelteret and Reddy (2012)		
	Rho et al. (1993)		
Glandular soft	Carter et al. (2012)	$2.59 \times 10^3$	0.45
	Ramiao et al. (2016)		
Glandular stiff	Carter et al. (2012)	$3.39 \times 10^4$	0.45
	Ramiao et al. (2016)		
Muscle soft	Chen et al. (1996)	$4.16 \times 10^3$	0.45
	Gennison et al. (2010)		
	Huang et al. (2007)		
Muscle medium stiff	Kajee et al. (2013)	$2.44 \times 10^4$	0.45
	Mathur et al. (2001)		
	Morrow et al. (2010)		
Muscle stiff	Gennison et al. (2010)	$5.34 \times 10^5$	0.45
	Morrow et al. (2010)		
	Yu et al. (2014)		
Mucosa soft	Sawada et al. (2011)	$2.3 \times 10^5$	0.45
Mucosa stiff	Chen et al. (2015)	$2.75 \times 10^6$	0.45
	Yuko et al. (2015)		
Tendon	Carrigy et al. (2015)	$3.9 \times 10^7$	0.45

The Young's modulus is the stiffness of the material. The Poisson ratio explains the contraction of the soft tissue material when an external pulling force is being exerted.

FE = finite element.

mucosal tissue were obtained from the works of Kuehn and Kahane, Eterna and Kuehn, Kuehn and Moon, and Cho et al.<sup>8-11</sup> All papers used to describe the parameters are stated in Table II. Soft tissues were modelled as hyperelastic whereas bone was modelled as linear elastic. The material parameters reported in the literature vary considerably. This is in accordance with the fact that the modulus of elasticity of one tissue type can vary significantly between individuals and even within one individual.<sup>15</sup> As a consequence, more than one set of material parameters was applied for each tissue type.

Previous modelling of the upper airways varies in complexity of geometry and material modelling. Two-dimensional models investigate the pharyngeal mechanisms in the mid-sagittal plane, however, they do not consider the influence of the lateral walls<sup>27</sup> (Berry et al. 1999, Huang et al. 2007). Three-dimensional models demonstrated that material modelling influences the response of the soft tissues when loads were applied (Pelteret et al. 2014, Zhao et al. 2013) but they are costly and are frequently based on single-patient CT or MRI data.

## MATERIAL MODEL

The mechanical behavior of soft tissue is governed by the protein macromolecules elastin and collagen,

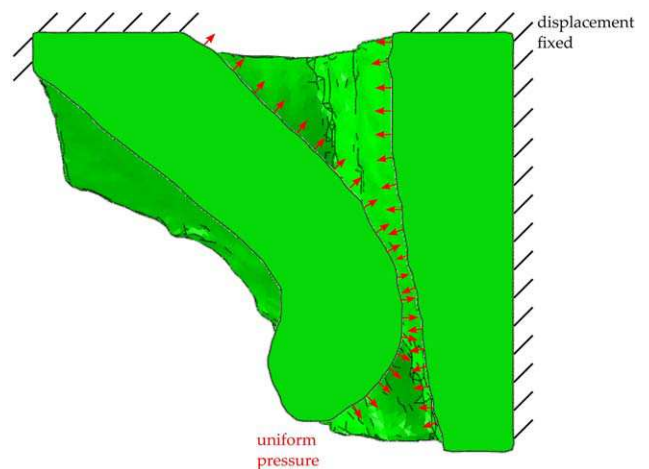


Fig. 2. Sketch of the boundary conditions. The boundaries of the model were chosen to match surfaces where soft tissue adheres to bone to ensure physically valid boundary conditions. A minimum of 4 mm soft tissue was included between the lateral airway walls and the lateral boundaries of the models.

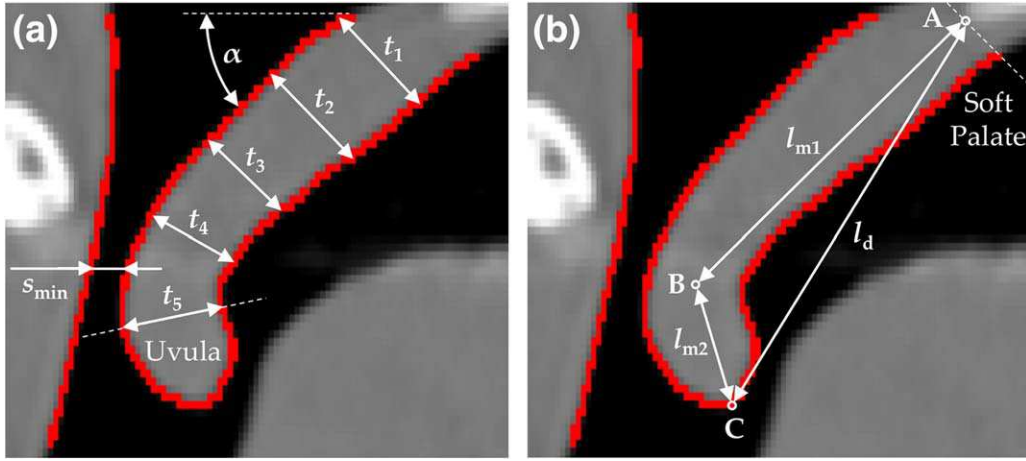


Fig. 3. A. Thickness and angle of the soft palate and the minimum airway space. The mean thickness ( $t_{\text{mean}}$ ) and the mean airway width ( $w_{\text{mean}}$ ) were calculated from five evenly distributed locations from the base of the hard palate to the base of the uvula. B. Measures of length of the soft palate.

which are present in the extracellular matrix. Elastin is the most linear elastic biosolid material. When subjected to loads, the stretching mechanism initially depends on elastin and there is no load on the collagen fibers yet. This leads to a quasilinear behavior at low strains where the loading curve is almost a straight line. Collagen is the main load-carrying element in soft tissues. As long as there is no load on the collagen fibers, they are at least partly in an amorphous configuration. With increasing loads, the collagen fibers start to bear loads and to straighten in the load direction. The material behavior is nonlinear during this process and the soft tissue stiffens significantly. When the collagen fibres are aligned, the stress strain relation becomes linear and the tissue is stiff compared to its stiffness under small loads.<sup>16–19</sup> For the physiological displacement levels of the soft palate the materials mainly operate in the linear regime, and for this the Neo-Hookean model is an acceptable first approach.<sup>17</sup> It is the simplest hyperelastic material model and the strain energy density function  $\Psi$  requires only two material parameters  $c_{10}$  and  $D_1$  that quantify the stiffness and the compressibility of the soft tissue, respectively.

$$\Psi = \frac{1}{2}c_{10}(I_1 - 3) + \frac{1}{D_1}(J_{el} - 1)^2$$

$I_1$  is the parameter that characterises the deformation and  $J_{el}$  is the elastic volume change.<sup>20,21</sup>

### FE Modelling and Posture/Gravity Loads

The displacement of the anterior, lateral, posterior, and proximal side of the FE model was set to zero to model the restriction of the hard palate, the cervical spine, and other tissues on the deformation of the soft tissues of the upper airway (Fig. 2). C3D10H elements (used in stress analysis to simulate incompressible materials) were applied to prevent unnatural stiffening and to grant optimal simulation results. A gravitational load was used to model the difference between the upright and the supine position as most apnea events occur in the supine position.<sup>22,23</sup> The displacements of the soft palate due to a change from the upright to the supine position reported in the literature vary from 1.4 mm<sup>24</sup> to 2.36 mm,<sup>25</sup> the average displacement being 2.02 mm. The computed displacements resulting from supine to

TABLE III.

Maximum Airway Widening Due to Gravity for Different Neo-Hookean Material Models in the Homogeneous and Layered Model and Mixed Model.

	Material model	Patient 1 (mm)	Patient 2 (mm)	Patient 3 (mm)	Patient 4 (mm)	Patient 5 (mm)	Patient 6 (mm)
Homogeneous model	Soft	7.80	15.25	15.83	2.35	5.60	9.16
	Medium	1.31	2.79	3.81	0.27	0.71	1.34
	Stiff	0.53	0.88	1.21	0.09	0.23	0.42
Layered model	Soft	0.45	0.56	1.1	0.42	0.43	0.68
	Medium	0.041	0.048	0.11	0.031	0.16	0.066
	Stiff	0.026	0.033	0.055	0.018	0.067	0.033
Mixed model	Soft	1.65	3.35	4.54	0.38	0.98	1.66
	Medium	1.07	2.43	3.28	0.21	0.59	1.09

Reported average airway widening in the literature is 2.0 mm.

TABLE IV.  
Patient Demographics.

P	G	BMI	Thickness (mm)	Width (mm)	S <sub>min</sub> (mm)	Area (mm <sup>2</sup> )	Volume (mm <sup>3</sup> )	AHI pre	AHI post	P <sub>crit</sub> (cm H <sub>2</sub> O)
1	m	33.1	9.1 ± 1.0	21.8 ± 1.5	1.1	968 ± 86	8812 ± 1262	41	30.7	-1.2
2	m	25.9	6.5 ± 0.5	24.2 ± 4.1	1.0	1060 ± 182	6890 ± 1275	19.1	15.2	-0.4
3	m	25.2	6.5 ± 0.5	29.8 ± 4.2	0.3	1475 ± 209	9589 ± 1543	50.1	53.4	-0.1
4	f	27.0	8.5 ± 1.2	13.3 ± 6.0	0.5	573 ± 260	4851 ± 2306	18.1	19.2	-4.1
5	m	24.3	9.4 ± 0.8	23.0 ± 6.1	0.8	1014 ± 275	9514 ± 2709	18.0	5.6	-1.9
6	m	26.9	9.1 ± 0.9	22.7 ± 3.6	0.4	891 ± 153	8110 ± 1603	11.1	3.1	-0.7

Geometry of the soft palate, minimal airway space (S<sub>min</sub>), baseline and postoperative values of the apnea-hypopnea-index (AHI) and critical closing pressure (P<sub>crit</sub>).

BMI = body mass index; G = gender; P = Patient number.

upright position presented in Table III are compared to this value in order to have a guide on what material parameter set is most representative. Negative intraluminal pressure during inspiration narrows the airway and might lead to airway collapse.<sup>26-28</sup> As the displacement of the soft palate is governed by air pressure with minimal influence of shear forces,<sup>29</sup> the load on the soft palate during inspiration was modelled as a uniformly distributed negative pressure. The distance from the soft palate to the pharyngeal wall was monitored during the Abaqus simulations. The closing pressure was identified as the pressure when the distance between the soft palate and the wall was below a very small value, ie, a simplification avoiding performing contact analysis.

## RESULTS

The patient demographics and geometric values of the soft palate, the apnea-hypopnea-index (AHI) and minimal airway space are listed in Table IV. The table also provides the computed critical closing pressures.

### *The Homogenous Soft Palate Model*

Finite element simulations were conducted with a soft, medium, and a stiff Neo-Hookean material model (Tables (I-III), II, and III). The medium stiff homogeneous model is the most accurate choice of model to evaluate gravitational deformation, compared to literature.<sup>25</sup> The displacement due to gravity may be used to measure the effect of individual anatomy on soft palate

TABLE V.  
Goodness-of-Fit Measures for the Soft Palate.

	Measure	SSE	R-square	RMSE	ŷ
Influence of anatomy on tissue deformation due to gravity	t <sub>mean</sub>	2.32	0.74	0.76	8.2 mm
	l <sub>d</sub>	19.31	0.81	2.20	41.9 mm
	l <sub>mid</sub>	32.27	0.41	2.84	44.1 mm
	w <sub>mean</sub>	40.32	0.72	3.18	22.5 mm
	u <sub>mean</sub>	5.19	0.18	1.14	6.4 mm
	V	1.40 × 10 <sup>7</sup>	0.16	1.87 × 10 <sup>3</sup>	7.96 × 10 <sup>3</sup> mm <sup>3</sup>
	Shape factor l <sub>mid</sub>	993.62	0.94	15.28	128.38 mm
	Shape factor l <sub>d</sub>	718.52	0.96	13.40	123.90 mm
	Influence of anatomy on closing pressure	t <sub>mean</sub>	7.06	0.20	1.33
l <sub>d</sub>		59.24	0.43	3.85	41.9 mm
l <sub>mid</sub>		51.06	0.06	3.57	44.1 mm
w <sub>mean</sub>		22.61	0.84	2.38	22.5 mm
U <sub>2,max</sub> linear fit		3.21	0.64	0.90	1.7 mm
U <sub>2,max</sub> exp.fit		0.87	0.90	0.54	1.7 mm
b <sub>min</sub>		0.55	8.3x10 <sup>-4</sup>	0.37	0.7 mm
A		1.43 × 10 <sup>5</sup>	0.66	189.15	997.2 mm <sup>2</sup>
Shape factor l <sub>mid</sub>		7.43 × 10 <sup>3</sup>	0.55	43.11	128.3 mm
Shape factor l <sub>d</sub>	7.89 × 10 <sup>3</sup>	0.57	44.41	123.8 mm	

FE simulations of the influence of anatomical measures on tissue deformation and closing pressure. ŷ reflects the mathematical expectations of the anatomical features.

A = area; b<sub>min</sub> = minimal airway space; FE = finite element; l<sub>d</sub> = length direct. l<sub>mid</sub> = length midline; t = thickness; u = uvula length; U<sub>2</sub> = maximal deformation; V = volume; w = width

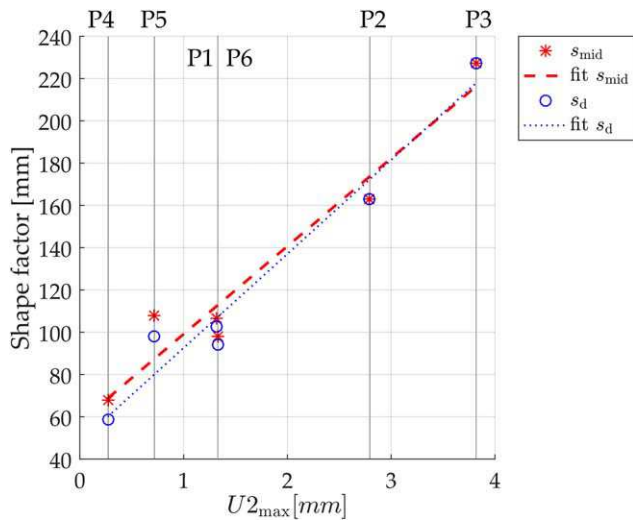


Fig. 4. The shape factor of the soft palate and maximal displacement ( $U_{2,max}$ ) due to gravity. Red asterisk and line = shape factor using the midline length ( $s_{mid}$ ). Blue circle and line = shape factor using the direct length ( $s_d$ ).

stiffness and tissue deformation. The mean thickness, direct length, and mean width of the soft palate were separately good fits to the FE model (Table IV). In order to predict the effect more accurately we constructed a “shape factor.” A shape factor of the soft palate is determined by the product of its length and width divided by its thickness:  $s = l \cdot w_{mean}/t_{mean}$ . Since the sagittal shape of the soft palate is angled at the base of the uvula we determined to types of soft palate lengths, the midline length ( $l_{mid}$ ) and the direct length ( $l_d$ ) (Figs. 3A and 3B). Compared to using the volume of the soft palate, the shape factor yielded a good correlation with the maximal displacement of the soft palate due to gravitational loads with the  $l_d$  giving a marginally better fit than  $l_{mid}$  (Table V, Fig. 4). The length of the uvula and the volume of the

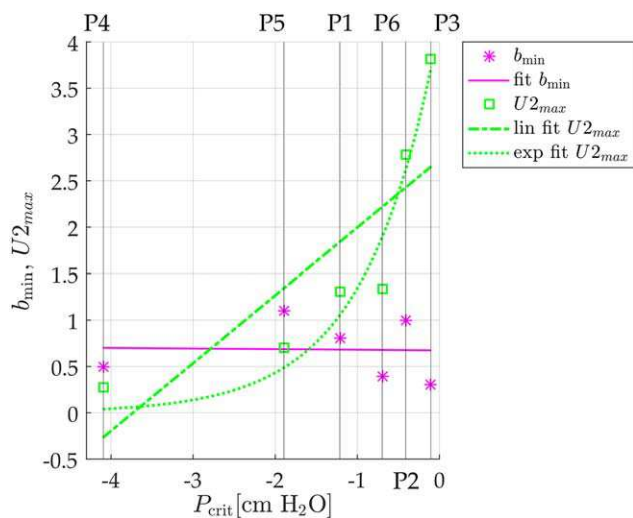


Fig. 5. Minimum airway space ( $b_{min}$ ), maximal displacement due to gravity ( $U_{2,max}$ ) and closing pressure. The maximal displacement has a relationship to closing pressure of a higher order, possibly exponential.

soft palate had a poor goodness of fit measure, indicating a weak relationship between uvula length and soft palate volume and tissue displacement (Table V). One interesting feature in our simulations was that the maximal displacement of the soft palate might be an indicator for soft palatal compliance and seemed to have a relationship to closing pressure that was of a higher order (Fig. 5), but with only six simulations the results are still uncertain.

In the FE model, the displacement of the soft palate at the critical closing pressure ( $P_{crit}$ ) could be visualized. The maximal displacement can be seen at the tip of the uvula, but the location of the airway obstruction was at the level of the lateral attachment to the pharyngeal wall rather than at the distal end of the soft palate in five of six patients (Figs. 6 and 7). The influence of the soft palate anatomy on closing pressure was considered in the same manner as with gravitational loads. The single most reliable fit of the anatomic measures on the closing pressure was the width of the soft palate (Fig. 8).

### The Layered Soft Palate Model

The displacement of the soft tissue due to gravity in the layered model was extremely small due to the stiffness of oral mucosa used in the model. Adipose soft tissue, musculature, and glandular soft tissue are comparable in stiffness to the medium homogeneous model, while the oral mucosa is at least one order of magnitude stiffer than the medium homogeneous model. The material parameters for oral palatal mucosa in the literature are from the masticatory mucosa lining the dorsum of the tongue, hard palate, and gingiva, and unsuitably stiff for modelling the soft palate. We replaced the material parameters of the oral mucosa with the values for the medium homogeneous model and let the other soft tissue parameters remain, thus creating a new mixed layered model (Table II). The layered soft palate model is therefore not able to describe the material properties of the soft palate appropriately and reflects the lack of sufficient experimental data for soft palate mucosa. The effect of the different compositions of soft tissue on the closing pressure is illustrated in Figure 9. It reveals a more profound difference between the material models in patients with a more negative closing pressure. The higher the closing pressure, and thus the more compliant the soft palate becomes, the less the composition of the soft tissue seems to matter. Similar to the homogeneous model, the airway occlusion is primarily at the level of the lateral attachment of the soft palate to the pharyngeal wall.

### Strain

The total transverse strain of the soft palate, defined as the posterior mid-sagittal point with the highest strain (LE11), correlates strongly with the closing pressure (Figs. 10 and 11) with an R-square of 0.92. A less negative closing pressure corresponds to small strain in the transverse direction. The strains in the LE22 and LE33 direction did not show the same degree of linearity as LE11, with an R-square of 0.88 and 0.68,

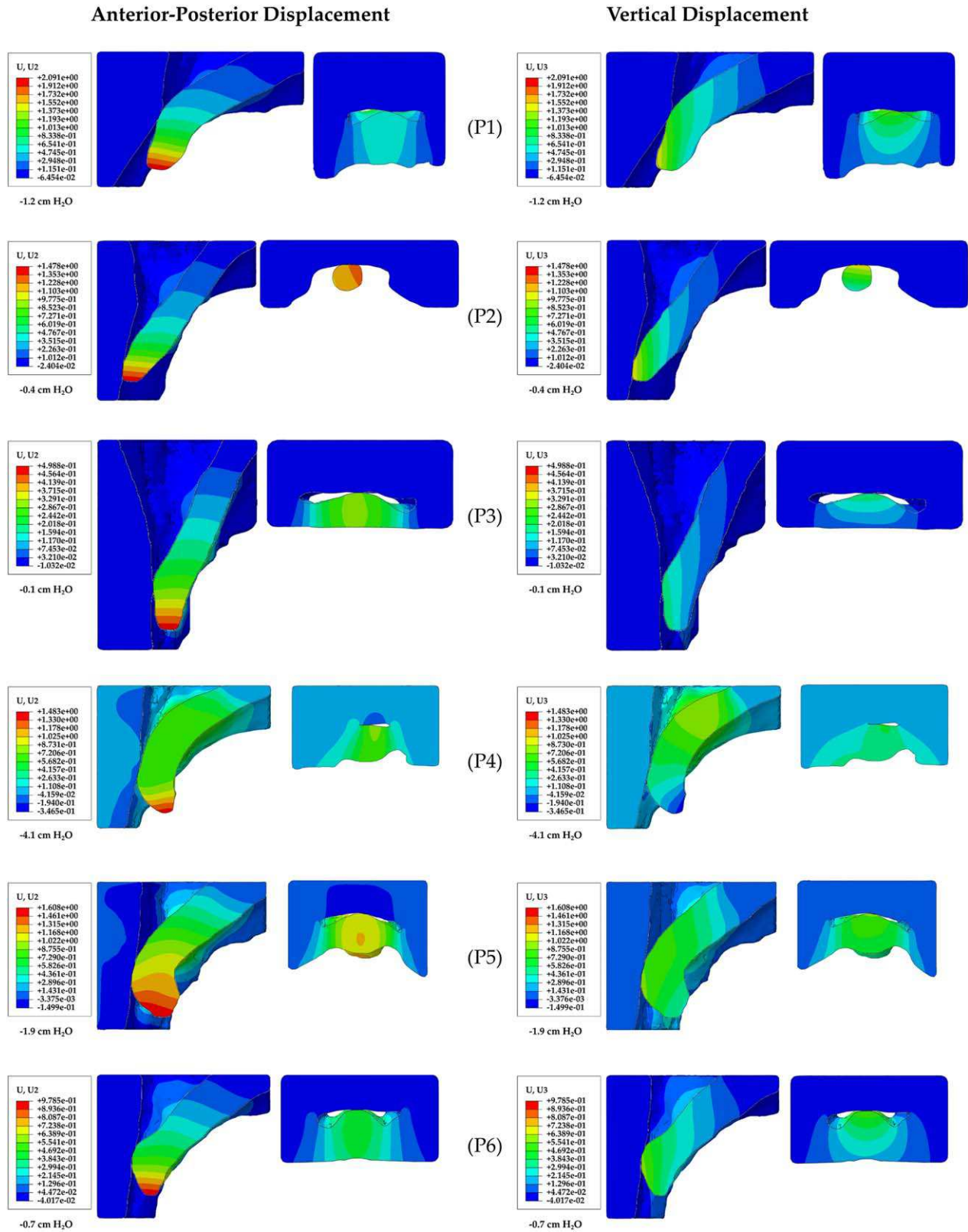


Fig. 6. Displacement of the soft palate in the anterior-posterior direction (figures on the left), and in the vertical direction (figures on the right). Patient numbers 1–6 from top to bottom (P1–P6).

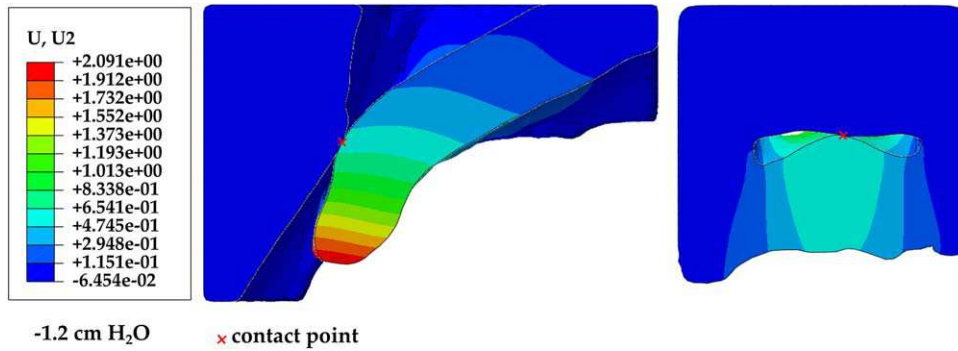


Fig. 7. Point of contact between the velopharynx and the posterior pharyngeal wall in the sagittal and axial plane, defining the simulated closing pressure in the FE models.  
FE = finite element

respectively. For LE22 maximum strain values were situated at the anterior (oral) part of the soft palate for most of the patients and were generally smaller than the maximum transverse strain. Based on the histology study by Ettema and Kuhn, the palate has a layered structure with a dominating collagen and muscle fiber orientation in the transverse direction.<sup>8</sup> For low tensile strains the collagen fibers are curved (wavy) and do not carry any significant stress. Almost all biological soft tissues with collagen fibers embedded in an extracellular matrix show a “knee point” in the stress versus strain curve, eg, Gasser et al., 2006 and Skallerud et al., 2011.<sup>30,31</sup> Prior to this point, elastin provides some resistance to strain. After this point, the collagen fibers straighten out and provide a significant increase in resistance to straining. Although our simulations are based on a simplified hyperelastic material model that does not account for the collagen, the strain levels computed in the palates are in the low range where stiffness is governed by elastin. Hence, our material model is representative. Figure 10 demonstrates that the maximal

transverse strain is mainly located at the area of obstruction, and not at the area of maximal displacement.

### The Minimal Airway Space

The minimum airway space was defined from the CT scans in each patient as the minimum length from the dorsal side of the soft palate to the posterior pharyngeal wall. The subsequent minimal airway space ( $b_{min}$ ) in the FE models was also determined for each patient. In contrast to assumption there was no obvious relation between  $b_{min}$  and  $P_{crit}$ , with an extremely small R-square (Table V) indicating that airway diameter alone is not sufficient to predict airway collapse.

### Effect of Nasal Surgery on the Soft Palate

The overall reduction of AHI in the group was 19.2%. Surgical success defined as a decrease in AHI of 50% or more was achieved in two out of six patients. Four patients achieved a decrease in AHI by 20% or

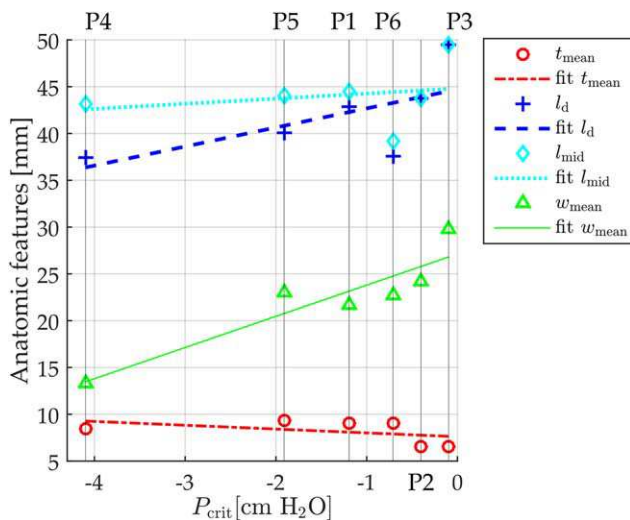


Fig. 8. Individual anatomic measures of the soft palate and closing pressure. Patients sorted by ascending closing pressure. The mean width (green triangle and line) is the only anatomic measure that yields a reasonable goodness of fit.

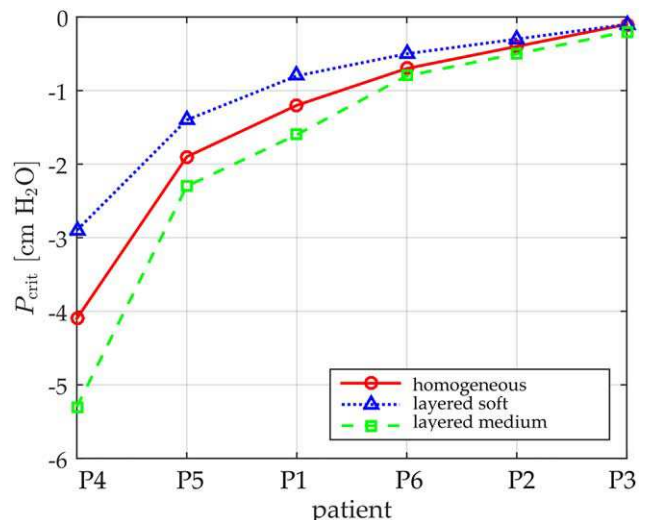


Fig. 9. Closing pressure in the supine position for different material models. Increasing closing pressure corresponds to increasing compliance of the soft palate.



## Total Transverse Strain

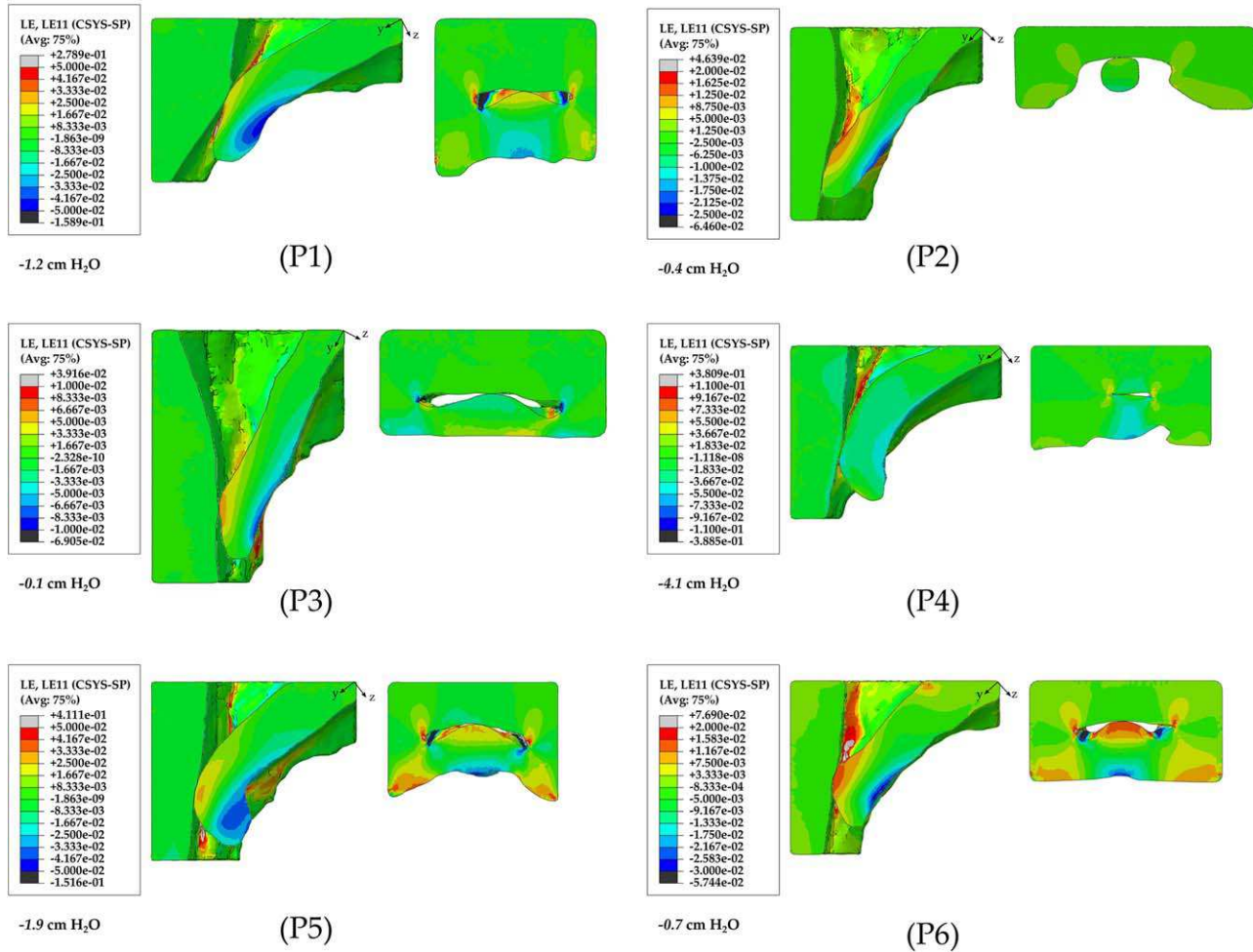


Fig. 10. Total strain in the lateral to lateral direction. Sagittal plane to the left, axial plane to the right. Patient number 1–6 from top to bottom (P1–P6).

more, and two patients experienced a worsening of the condition defined as an increase in AHI by 6%. The  $P_{crit}$  and the medical data of preoperative AHI level showed no linear relationship. Similarly, the  $P_{crit}$  did not show a linear relationship to change in AHI after nasal surgery. A high AHI does not necessarily translate into a high (less negative) simulated  $P_{crit}$  and as a consequence the FE-model of the soft palate and velopharynx does not seem to be a suitable tool to predict the severity of OSA or the outcome on OSA after nasal surgery.

## DISCUSSION

Our FE models indicate that the individual shape of the soft palate influences the closing pressure and the stiffness of the soft tissue in the velopharynx. The evaluation of passive mechanical behaviour of the soft tissues in the upper airway is challenging because there will be a neural driving mechanism in the airway musculature. Pelteret and Reddy demonstrated in 2013 a considerable difference in the displacement of the tongue due to gravity in their FE model depending on whether active

muscle control was applied or not.<sup>30,32</sup> Studies of paralyzed human airways, however, demonstrate that the upper airways in OSA patients are more compliant than in healthy subjects suggesting that geometric characteristics alone can influence the biomechanical response of the airway.<sup>33,34</sup> The shape factor of the soft palate influences the tissue gravitational displacement in a positive linear fashion and may be used as a way of determining the level of tissue deformation due to posture in OSA patients. Even though the mean thickness, length, and width clearly shows a positive correlation to tissue displacement, the combined value of the shape factor seems to be more accurate (Fig. 4). The notion of a shape factor based on combined geometric values may be applied to other defined anatomical sites in the airway, ie, the tongue or even the total pharyngeal soft tissue compartment. The length of the uvula and the volume of the soft palate both have an inappropriate fit and are unable to explain the degree of displacement of the soft palate.

The concept of the critical closing pressure ( $P_{crit}$ ) is widely used as a means to describe the collapsibility of the airway.<sup>1,35</sup> However, the upper airways cannot

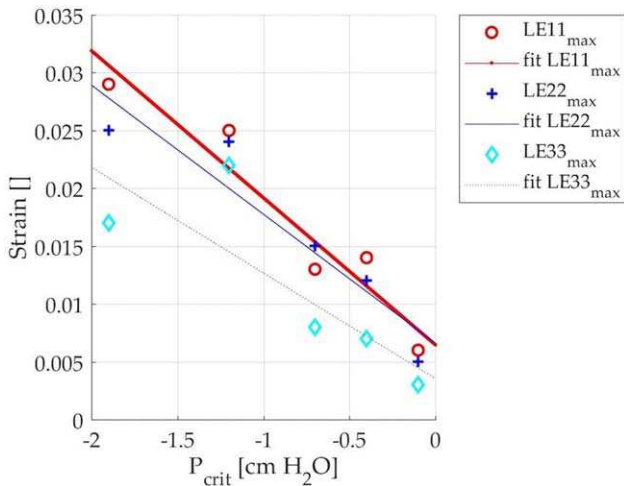


Fig. 11. Strains and closing pressure. LE11 (red circles and line) shows a better linear fit than LE22 and LE33. One should note that although a linear correlation between strain and pressure is obtained, the linear curve does not go through the origin. Hence, one should be careful in using this result for closing pressures near zero. The palatal load for patient 4 is mainly dominated by shear stresses and bending stresses and is therefore not included in the plot.

automatically be explained by a Starling resistor mechanism, because it does not take into account the muscle activity and biomechanical qualities of the velopharynx.<sup>36</sup> The minimum airway space is insufficient to predict the collapse of the upper airway and may be caused by the fact that the displacement of the soft palate is not merely in the anterior-posterior direction but has a vertical component as well. Even though the maximal displacement is at the distal end of the soft palate, the FE models show that the airway occlusion is at the level of the lateral attachment of the soft palate to the pharyngeal wall in all but one case. Consequently, surgical procedures involving the soft tissue in the distal part of the soft palate are likely to have a limited impact on closing pressure and the development of apneas, which is consistent with the repetitively low success scores of soft palate surgery on OSA outcome.<sup>37,38</sup> Similar to the effect of gravity on tissue deformation, the length of the uvula and the volume of the soft palate do not show a linear relationship to the closing pressure. Of all the anatomical landmarks, it seems that the mean width of the soft palate is the most likely anatomical landmark that can be correlated to the critical closing pressure. The shape factor is not a predictor of closing pressure. However, the maximal displacement of the soft palate may have a relationship to the closing pressure that is not linear, but of a higher order, possibly exponential (Fig. 5 and Table V). A bigger sample size is necessary to identify the maximal displacement as an indicator of soft palate compliance and critical closing pressure (Fig. 4). The macro anatomy seemed to have a more substantial influence in patients with a less negative closing pressure, while the effect of the difference in soft tissue composition was more pronounced in patients with a stiffer soft palate and a more negative closing pressure (Fig. 6).

Difference in soft tissue composition may therefore have a larger clinical impact in social snoring or patients with mild to moderate OSA than in patients with more severe upper airway collapse. It does not, however, mean that the layered model is inferior to the homogeneous model in severe OSA. Rather it points to other areas of the upper airway that may contribute to the disease in severe cases of OSA.

There seems to be a strong correlation between total transverse strain and closing pressure in our models (Fig. 11). In our model, the soft palate resembles a plate that is fixed at three sides (hard palate anteriorly, bony attachments to each lateral side) and free at the fourth distal end in the direction of the uvula. In the mid-sagittal plane, the boundary conditions resembles a cantilever type, and the strain is dominated by bending strain due to the curvature along the longitudinal y-axis (LE22). In the transverse plane, due to the boundary conditions, the strain will be a combination of bending (due to the curvature along the transverse x-axis) and membrane tension (LE11). In this transverse plane, membrane strain in the longitudinal y-axis (LE22) does not develop as the distal uvula end is free. Thus, the strain along the transverse axis (LE11) was of largest interest and was used to check for correlation against closing pressure. This also has a link to the anatomical measure of soft palate width, that showed a correlation to closing pressure.

The strain along mid thickness in the lateral to lateral direction describes mainly membrane strain. In some patients, we saw a tensile membrane strain on the posterior side of the soft palate, but a compressive strain on the anterior side. This can probably be explained by an additional large bending contribution as well, meaning that there is a curvature in both the x and y direction giving bending strains in both directions. The membrane strain at mid thickness is superposed to this (on the posterior side the curvature in the y-direction gives a tensile bending strain in addition to tensile membrane strain. On the anterior side the curvature gives a compressive bending strain that is superposed to the membrane strain). The total transverse strain is the dominant strain components except in patients 2 and 4. In patient 2, bending strain and membrane strain have approximately the same order of magnitude (therefore maximum principal strain seems to be compression at both sides of the soft palate), but the total strain value fits the linearity when plotted versus closing pressure. In patient 4, the closing of the airway occurs very close to the attachment of the soft palate to the lateral airway walls. One can also note that the soft palate width in this patient is about half the size of the others (Table III). This leads to the upper airway negative pressure being carried to a much larger extent by shear stresses and bending stresses, ie, the transverse membrane stress and strain are less compared to the other patients. Since the strain cannot be regarded as a measure of total transverse strain this case is not included in Figure 11. It should be mentioned that we neglect any neuromuscular activation. The striated muscle fibers in the palate provides a contraction reflex when the palate

approach closure. Studies show that this reflex and corresponding activation level is significantly reduced compared to healthy persons, as reported previously.<sup>39,40</sup> Not accounting for the reduced muscle activation in sleep apnea patients may be considered as a conservative approach to predict the closing pressure. Further studies should be carried out in order to resolve this issue.

Surgery of the distal part of the soft palate as an isolated procedure is no longer advised<sup>41</sup> due to unsatisfactory results with failure in 40–60%<sup>42</sup> and long-term side effects such as dysphagia, globulus sensation, velopharyngeal insufficiency, and xerostomia in a mean of 58% of the patients.<sup>43,44</sup> This is consistent with our results in that the distal part of the soft palate does not seem to be the most prominent site of obstruction when it comes to high obstructions.

We found no correlation between minimum airway space and the critical closing pressure (Table V). The exact positioning of the lower jaw during medical imaging can influence the minimal airway space of the upper airways and no standard method has been introduced to minimize bias in this regard. The impact of observed airway space should therefore not be relied upon to give solid information on the degree of obstruction in the velopharyngeal area. In order to reduce such systematic error, we had all patients fitted with a 20-mm mouth-piece during the imaging procedures.

Nasal surgery relieves symptoms in most OSA patients<sup>45,46</sup> and is known to reduce the number of apneas to some degree.<sup>47</sup> However, no guidelines exist as to what type of nasal surgery to perform and no method is available to predict the surgical outcome. In addition to increasing the compliance for pressure devices, the surgical alterations in the nasal cavity are reported to reduce the AHI by 50% in 15% of the patients.<sup>47,48</sup> We found an average reduction in AHI of 19.2% and a surgical success in 33% three months after nasal surgery. All patients had septoplasty and turbinectomy performed. There was no correlation between simulated  $P_{crit}$  and preoperative AHI in our study. The patient with the highest AHI preoperatively also had the least negative simulated  $P_{crit}$ , which could have been an indication of a relationship between the preoperative AHI values and the FE model. However, none of the other patient data gave support to this view. This suggests that the effect on OSA outcome in nasal surgery is more likely dependent on the structural intranasal alterations induced by the surgery itself or on changes in other parts of the upper airway secondary to the restoration of nasal patency, possibly by inducing a switch from oral to nasal breathing which enables normal muscular neuroregulation in the pharynx as well as creating a larger antero-posterior diameter in the retroglottic area.<sup>48,49</sup> It is worth mentioning that our patients had surgery done in the anterior part of the nasal cavity which includes the posterior part of the nasal vault, which may be an area of importance in OSA patients.<sup>50</sup> Since nasal surgery does create change in the upper airway compliance, it may be used as a tool to investigate the changes in upper airway biomechanics using FE simulations. A FE model that comprises solely one anatomic feature seems

to be insufficient to comprehend all relevant effects of OSA. A more extensive model including the nasal cavity, the soft palate, the tongue, the epiglottis and the hypopharynx might increase modelling accuracy.

Even though the soft palate is the most important site of airway collapse in patients with oropharyngeal obstructions,<sup>35</sup> its biomechanical properties are less researched and it is usually modelled as linear-elastic and homogeneous, instead of hyperelastic, nonlinear and heterogeneous. The available full 3D models are usually expensive to conduct and in most cases the data is derived from a single patient. A larger study population will therefore be necessary to obtain clinically valid data.

### **Strengths and Limitations**

The hyperelastic and nonlinear model of the velopharynx and soft palate represents a new approach to evaluate the biomechanics of the upper airways. Former research on the topic is scarce, and 3-D simulations are mostly confined to single patient studies due to high computational costs. The inclusion of six patients enhances the chances of creating a more reliable model, and an even larger study population would be preferable. However, the FE models are only an approximation of the actual anatomic site and velopharyngeal function. Larger study populations that include the hypopharynx and larynx are needed in order to verify the relationship between upper airway anatomic landmarks, maximum deformity of the soft tissue, total transverse strain and  $P_{crit}$ . In particular the relation between anatomical features versus membrane strain and bending strain needs further studies with larger cohorts. The resolution of the CT scans restricts the FE models, and particularly the study of histologic structures. The relationship between the solid soft tissues and the fluid within the airways have not been investigated, hence the influence of fluid-structure interaction is not accounted for.

### **CONCLUSION**

Our FE simulations indicate a correlation between anatomic measures, displacement of the soft palate, and OSA, as well as a correlation between total transverse strain of the soft palate and closing pressure. Previous modelling of the soft palate does not take into account the hyperelastic properties of the soft palate, or the possible effects of the different soft tissues that constitute the palate or the forces caused by its lateral attachment to the pharyngeal wall. FE simulations applying hyperelastic, nonlinear, and heterogeneous material models show that the primary site of obstruction of the soft palate in OSA is at the level of the lateral attachments rather than at the distal part of the soft palate, and this observation may explain the relatively low success rate observed in single soft palate surgery in OSA patients. The closing pressure is correlated to total transverse strain and FE simulations may represent a possible way to predict closing pressure in the velopharynx, but the possible interaction of neuromuscular activation on strain should be accounted for in future studies. The FE

simulations indicate that the soft palate may not represent the primary site of critical closing pressure in OSA after nasal surgery. FE models of larger sections of the upper airway are needed to predict  $P_{crit}$  and OSA severity more accurately. Soft tissue biomechanics and fluid structure interaction will be of increasing importance in the planning of surgical interventions in obstructive sleep apnea and upper airway disorders.

## BIBLIOGRAPHY

- Bilston LE, Gandevia SC. Biomechanical properties of the human upper airway and their effect on its behavior during breathing and in obstructive sleep apnea. *J Appl Physiol* (1985) 2014;116(3):314–324.
- Steward DL, Huntley TC, Woodson BT, Surdulescu V. Palate implants for obstructive sleep apnea: multi-institution, randomized, placebo-controlled study. *Otolaryngol Head Neck Surg* 2008;139(4):506–510.
- Takahashi R, Ohbuchi T, Hohchi N, et al. [Effect of septoplasty and turbinectomy on obstructive sleep apnea syndrome]. *Nihon Jibiinkoka Gakkai Kaiho* 2013;116(7):789–792.
- De Kermadec H, Blumen MB, Engalenc D, Vezina JP, Chabolle F. Radiofrequency of the soft palate for sleep-disordered breathing: a 6-year follow-up study. *Eur Ann Otorhinolaryngol Head Neck Dis* 2014;131(1):27–31.
- Holmlund T, Levring-Jaghagen E, Franklin KA, Lindkvist M, Berggren D. Effects of radiofrequency versus sham surgery of the soft palate on daytime sleepiness. *Laryngoscope* 2014;124(10):2422–2426.
- Virk JS, Nouraei R, Kotecha B. Multilevel radiofrequency ablation to the soft palate and tongue base: tips and pitfalls. *Eur Arch Otorhinolaryngol* 2014;271(6):1809–1813.
- Brenner Scott L. *The Mathematical Theory of Finite Element Methods*. 1st ed. New York: Springer; 2011.
- Ettema SL, Kuehn DP. A quantitative histologic study of the normal human adult soft palate. *J Speech Hear Res* 1994;37(2):303–313.
- Kuehn DP, Kahane JC. Histologic study of the normal human adult soft palate. *Cleft Palate J* 1990;27(1):26–34; discussion 5.
- Kuehn DP, Moon JB. Histologic study of intravelar structures in normal human adult specimens. *Cleft Palate Craniofac J* 2005;42(5):481–489.
- Cho JH, Kim JK, Lee HY, Yoon JH. Surgical anatomy of human soft palate. *Laryngoscope* 2013;123(11):2900–2904.
- Birch MJ, Srodon PD. Biomechanical properties of the human soft palate. *Cleft Palate Craniofac J* 2009;46(3):268–274.
- Pirnar J, Dolenc-Groselj L, Fajdiga I, Zun I. Computational fluid-structure interaction simulation of airflow in the human upper airway. *J Biomech* 2015;48(13):3685–3691.
- Yu S, Sun XZ, Liu YX. Numerical analysis of the relationship between nasal structure and its function. *ScientificWorldJournal* 2014;2014:581975.
- Chen J, Ahmad R, Li W, Swain M, Li Q. Biomechanics of oral mucosa. *J R Soc Interface* 2015;12(109):20150325.
- Holzappel GA. Biomechanics of soft tissue. [Online]. Available at: [https://biomechanics.stanford.edu/me338/me338\\_project02.pdf](https://biomechanics.stanford.edu/me338/me338_project02.pdf). Accessed March 17, 2017.
- Freutel M, Schmidt H, Durselen L, Ignatius A, Galbusera F. Finite element modeling of soft tissues: material models, tissue interaction and challenges. *Clin Biomech (Bristol, Avon)* 2014;29(4):363–372.
- Fung YC. *Biomechanics: Mechanical Properties of Living Tissues*. 2nd ed. New York: Springer-Verlag; 1993. xviii, 568.
- Humphrey J. Review paper: continuum biomechanics of soft biological tissues. *Proc Royal Soc A* 2003;459(2029):3–46.
- Marckmann G, Verron E. Comparison of hyperelastic models for rubber-like materials. *Rubber Chem Technol* 2006;79(5):835–858.
- Dassault Systèmes. *Abaqus 6.14 Theory Guide: Hyperelastic Material Behavior*. Providence, RI: Dassault Systèmes Simulia Corp.; 2014.
- Park J, Ramar K, Olson E. Updates on definition, consequences, and management of obstructive sleep apnea. *Mayo Clin Proc* 2011;86(6):549–555.
- Oksenberg A, Silverberg D, Offenbach D, Arons E. Positional therapy for obstructive sleep apnea patients: a 6-month follow-up study. *Laryngoscope* 2006;116(11):1995–2000.
- Yildirim N, Fitzpatrick M, Whyte K, Jalleh R, Wightman A, Douglas N. The effect of posture on upper airway dimensions in normal subjects and in patients with the sleep apnea/hypopnea syndrome. *Am Rev Respir Dis* 1991;144(4):845–847.
- Pae E, Lowe A, Sasaki K, Price C, Tsuchiya M, Fleetham J. A cephalometric and electromyographic study of upper airway structures in the upright and supine positions. *Am J Orthod Dentofacial Orthop* 1994;106(1):52–59.
- Strohl K, Butler J, Malhotra A. Mechanical properties of the upper airway. *Compr Physiol* 2012;2(3):1853–1872.
- Huang Y, White D, Malhotra A. The impact of anatomic manipulations on pharyngeal collapse. *Chest* 2005;128(3):1324–1330.
- Malhotra A, Huang Y, Fogel R, et al. The male predisposition to pharyngeal collapse. *Am J Respir Crit Care Med* 2002;166(10):1388–1395.
- Zhu J, Lee H, Lim K, Lee S, Teo L, Wang D. Passive movement of human soft palate during respiration: a simulation of 3D fluid/structure interaction. *J Biomech* 2012;45(11):1992–2000.
- Gasser TC, Ogden RW, Holzapfel GH. Hyperelastic modelling of arterial layers with distributed collagen fibre orientations. *J Royal Soc Interface* 2006;3:15–35.
- Skallerud B, Prot V, Nordrum IS. Modeling active muscle contraction in mitral valve leaflets during systole: a first approach. *Biomech Model Mechanobiol* 2011;10:11–26.
- Pelteret JV, Reddy B. Development of a computational biomechanical model of the human upper-airway soft-tissues toward simulating obstructive sleep apnea. *Clin Anat* 2013;27(2):182–200.
- Isono S, Shimada A, Tanaka A, Ishikawa T, Nishino T, Konno A. Effects of uvulopalatopharyngoplasty on collapsibility of the retropalatal airway in patients with obstructive sleep apnea. *Laryngoscope* 2003;113(2):362–367.
- Isono S, Remmers JE, Tanaka A, Shio Y, Sato J, Nishino T. Anatomy of pharynx in patients with obstructive sleep apnea and in normal subjects. *J Appl Physiol* 1997;82:1319–1326.
- Dempsey J, Veasey S, Morgan B, O'Donnell C. Pathophysiology of sleep apnea. *Physiol Rev* 2010;90:47–112.
- Wellman A, Genta P, Owens R, et al. Test of the Starling resistor model in the human upper airway during sleep. *J Appl Physiol* 2014;117(12):1478–1485.
- Bäck L, Liukko T, Rantanen I, et al. Radiofrequency surgery of the soft palate in the treatment of mild obstructive sleep apnea is not effective as a single-stage procedure: a randomized single-blinded placebo-controlled trial. *Laryngoscope* 2009;119(8):1621–1627.
- Elshaug A, Moss J, Southcott A, Hiller J. Redefining success in airway surgery for obstructive sleep apnea: a meta analysis and synthesis of the evidence. *Sleep* 2007;30(4):461–467.
- Mezzanotte W, Tangel D, White D. Influence of sleep onset on upper airway muscle activity in apnea patients and control subjects. *Am J Respir Crit Care Med* 1996;153:1880–1887.
- McGinley B, Schwartz A, Schneider H, Kirkness J, Smith P, Patil S. Upper airway neuromuscular compensation during sleep is defective in obstructive sleep apnea. *J Appl Physiology* 2008;15:197–205.
- Friedman M, Wilson M. Re-defining success in airway surgery for obstructive sleep apnea. *Sleep* 2009;32:17.
- Väreth M, Berg S, Andersson M. Long-term follow-up of patients operated with uvulopalatopharyngoplasty from 1985 to 1991. *Respir Med* 2012;106:1788–1793.
- Franklin KA, Anttila H, Axelsson S, et al. Effects and side-effects of surgery for snoring and obstructive sleep apnea—a systematic review. *Sleep* 2009;32(1):27–36.
- Tang J, Salapatias A, Bonzelaar L, Friedman M. Long-term incidence of velopharyngeal insufficiency and other sequelae following uvulopalatopharyngoplasty. *Otolaryngol Head Neck Surg* 2017;156(4):606–610.
- Li H, Lin Y, Chen N, Lee L, Fang T, Wang P. Improvement in quality of life after nasal surgery alone for patients with obstructive sleep apnea and nasal obstruction. *Arch Otolaryngol Head Neck Surg* 2008;134(4):429.
- Michels Dde S, Rodrigues Ada M, Nakanishi M, Sampaio AL, Venosa AR. Nasal involvement in obstructive sleep apnea syndrome. *Int J Otolaryngol* 2014;717419
- Wu J, Zhao G, Li Y, et al. Apnea-hypopnea index decreased significantly after nasal surgery for obstructive sleep apnea: a meta-analysis. *Medicine (Baltimore)* 2017;96(5):e6008.
- Georgalas C. The role of the nose in snoring and obstructive sleep apnoea: an update. *Eur Arch Otorhinolaryngol* 2011;268(9):1365–1373.
- El Aouame A, Daoui A, El Quars F. Nasal breathing and the vertical dimension: a cephalometric study. *Int Orthod* 2016;14(4):491–502.
- Stupak H. Regarding “Does Nasal Surgery Improve OSA in Patients with Nasal Obstruction and OSA? A Meta-analysis” by Ishii et al, 2015. *Otolaryngol Head Neck Surg* 2016;154(3):575–575.